Cell Stress and Chaperones (2023) 28:773–785
https://doi.org/10.1007/s12192-023-01369-2

ORIGINAL ARTICLE

LED therapy plus idebenone treatment targeting calcium and mitochondrial signaling pathways in dystrophic muscle cells

Heloina Nathalliê Mariano da Silva[1] · Daniela Sayuri Mizobuti[1] · Valéria Andrade Pereira[1] · Guilherme Luiz da Rocha[1] · Marcos Vinícius da Cruz[1,2] · André Gustavo de Oliveira[1,2] · Leonardo Reis Silveira[1,2] · Elaine Minatel[1]

Received: 17 May 2023 / Revised: 20 July 2023 / Accepted: 7 August 2023 / Published online: 14 August 2023

Abstract

Intracellular calcium dysregulation, oxidative stress, and mitochondrial dysfunction are some of the main pathway contributors towards disease progression in Duchenne muscular dystrophy (DMD). This study is aimed at investigating the effects of light emitting diode therapy (LEDT) and idebenone antioxidant treatment, applied alone or together in dystrophic primary muscle cells from *mdx* mice, the experimental model of DMD. *Mdx* primary muscle cells were submitted to LEDT and idebenone treatment and evaluated for cytotoxic effects and calcium and mitochondrial signaling pathways. LEDT and idebenone treatment showed no cytotoxic effects on the dystrophic muscle cells. Regarding the calcium pathways, after LEDT and idebenone treatment, a significant reduction in intracellular calcium content, calpain-1, calsequestrin, and sarcolipin levels, was observed. In addition, a significant reduction in oxidative stress level markers, such as H_2O_2, and 4-HNE levels, was observed. Regarding mitochondrial signaling pathways, a significant increase in oxidative capacity (by OCR and OXPHOS levels) was observed. In addition, the PGC-1α, SIRT-1, and PPARδ levels were significantly higher in the LEDT plus idebenone treated-dystrophic muscle cells. Together, the findings suggest that LEDT and idebenone treatment, alone or in conjunction, can modulate the calcium and mitochondrial signaling pathways, such as SLN, SERCA 1, and PGC-1α, contributing towards the improvement of the dystrophic phenotype in mdx muscle cells. In addition, data from the LEDT plus idebenone treatment showed slightly better results than those of each separate treatment in terms of SLN, OXPHOS, and SIRT-1.

Keywords Dystrophic muscle cells · Photobiomodulation · Calcium signaling · Oxidative stress · Mitochondrial parameters

Introduction

Duchenne muscular dystrophy (DMD) is a genetic X-linked disease characterized by mutations of dystrophin protein, which leads to progressive muscle degeneration with a consequent loss of ambulation in adolescence and to death, at approximately 30 years of age, usually due to cardio-respiratory failure (Emery 2002; Landfeldt et al. 2018). There is currently no cure for DMD, and glucocorticoids are the main drug treatment used by dystrophic patients (Gloss et al. 2016). However, glucocorticoid continued use causes several adverse effects (Moxley et al. 2010), making it necessary to find new therapeutic approaches.

In addition to the primary genetic defect of DMD, the absence of dystrophin protein, several studies suggest that abnormal intracellular calcium concentration $[Ca^{2+}]_i$, reactive oxygen species (ROS), and mitochondrial dysfunction play a crucial role in the pathophysiology of this disease (Moore et al. 2020; González-Jamett et al. 2022).

Previous studies suggest that the sustained elevation of $[Ca^{2+}]_i$ underlies muscle pathology and dysfunction in DMD. Research showed that the increase of $[Ca^{2+}]_i$ enhances the expression and activity of calpains, the Ca^{2+}-dependent proteases in dystrophic muscles (Spencer et al. 1995; Hussain et al. 2000; Sundaram et al. 2006; Voit et al. 2017). Furthermore, it was also observed that increased $[Ca^{2+}]_i$ influences mitochondrial Ca^{2+} uptake, which in turn

✉ Elaine Minatel
minatel@unicamp.br

[1] Department of Structural and Functional Biology, Institute of Biology, University of Campinas, Campinas, Brazil

[2] Obesity and Comorbidities Research Center (OCRC), Campinas, Brazil

leads to altered metabolism and increased ROS production (Mareedu et al. 2021).

Mitochondria are the main source of ROS in dystrophic muscles (Moore et al. 2020). A recent study showed abnormal mitochondrial structure and reduced mitochondrial function in the dystrophic muscle of *mdx* mice (the experimental model of DMD), prior to the onset of muscle dystrophic fiber damage, suggesting an early mitochondrial role in the pathophysiology of DMD (Moore et al. 2020).

In search of alternative treatments for DMD, previous studies have pointed to the use of photobiomodulation (PBM) as a potential therapy (Silva et al. 2015; Macedo et al. 2020). PBM has presented several benefits in dystrophic muscles, such as the mitigation of inflammatory response and oxidative stress (Silva et al. 2015; Macedo et al. 2020). The effects of PBM result in the absorption of the light through the mitochondria, leading to an increase in membrane potential, the electron transport, and the oxygen consumption (Karu 2008; Freitas and Hamblin 2016). In this study, seeking to increase the therapeutic efficiency of PBM, we associated the PBM therapy (PBMT) with idebenone, a potent antioxidant and electron carrier. Idebenone is a synthetic short-chain benzoquinone, which improves mitochondrial function, restores ATP production, and reduces ROS (Buyse et al. 2015). In addition, recently, our research group showed that idebenone protected the dystrophic muscle cells by reducing the $[Ca^{2+}]_I$, oxidative stress, and inflammatory process (Valduga et al. 2023).

Thus, in the present study, we evaluated the LED therapy plus idebenone treatment effects in dystrophic muscle cells from *mdx* mice, focusing on the calcium and mitochondrial signaling pathways.

Materials and methods

Mdx primary muscle cells

The development of primary skeletal muscle cell cultures from *mdx* (C57BL/10-Dmdmdx/PasUnib) mice was based on protocol previously described (Rando and Blau 1994; Mizobuti et al. 2019). All the experiments were performed under an approved protocol of the Committee on the Ethics of Animal Experiments of UNICAMP (#5603-1/2020) and were in accordance with the Brazilian College for Animal Experimentation guidelines.

Experimental design (see Fig. 1)

LEDT

LEDT at 850 nm was applied on *mdx* primary muscle cells, using a ThorLabs Mounted High-Power equipment, and the parameters used (Table 1) are based on previous study (Rocha et al. 2022). The LEDT was applied to muscle cells at a perpendicular angle, by a single application, and irradiation was performed by one point at the center of each culture well. The cells were irradiated inside a laminar flow in a dark room without radiation. *Mdx* muscle cells not irradiated were used as control.

Idebenone treatment

The first experiment tried to establish the best dose of idebenone for *mdx* muscle cell proliferation by MTT assay. *Mdx* muscle cells received different doses of idebenone (0.5, 0.25, 0.12, 0.06, and 0.03 µM) diluted in 0.5% carboxymethylcellulose sodium salt (CMC, Fluka,

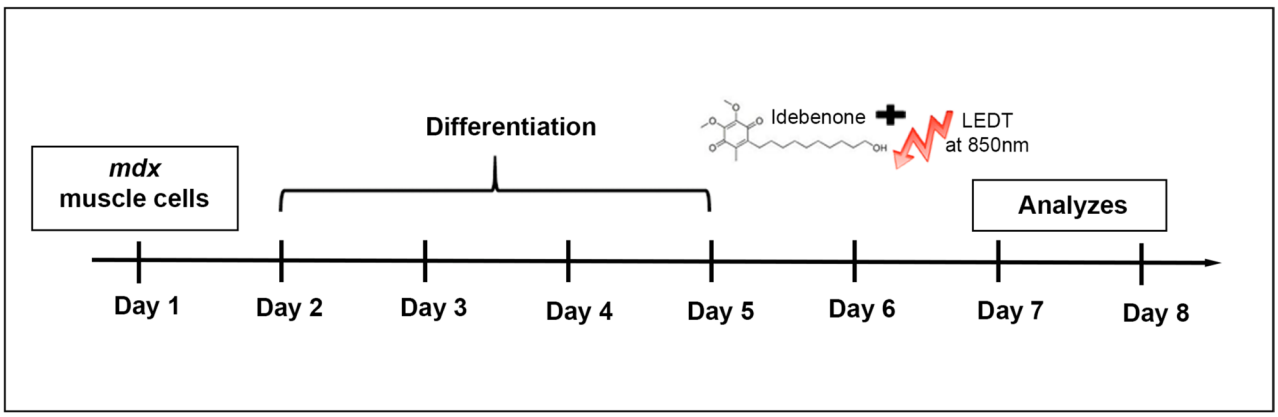

Fig. 1 Timescale of LEDT and idebenone treatment in *mdx* muscle cells

Table 1 Specifications of LEDT parameters

Device information		
Manufacturer	ThorLabs Mounted High-Power equipment	
Irradiation parameters	96 weels	6 weels
Output power (mW)	110	38
Spot size (cm^2)	0.32	9.5
Power density (w/cm^2)	343	4
Energy density (J/cm^2)	1.5	0.05
Time per point (s)	4.5	13.1
Wavelength (nm)	850	
Beam shape	Circular	
Operating mode	Continuous	
Number and frequency of treatment sessions	1	
Application technique	Applied directed to the cells through the bottom of each well	

Buchs, Switzerland) in water and were evaluated after 24 and 48 h of treatment. Subsequently, the *mdx* muscle cells received only two doses (0.06 and 0.03 µM; selected based on the results of MTT assay and IC50) and were evaluated after 24 and 48 h of treatment for cell viability (Neutral Red assay), $[Ca^{2+}]_i$, mitochondrial superoxide ($O2^{\bullet-}$), and H_2O_2 production analyses. Lastly, the other analyses were performed in *mdx* muscle cells treated with idebenone, after 48 h of treatment, at the chosen dose (0.06 µM). For all experiments, the untreated *mdx* muscle cells were used as controls.

Cell viability and proliferation

MTT analysis This colorimetric analysis was performed for quantification of cell metabolic activity. The protocol of this assay was previously described by Macedo et al. (2015) and Mizobuti et al. (2019). Briefy, after the MTT incubation phase, the crystals were dissolved with isopropanol acid, and the amount of formazan product was measured by a spectrophotometer (Synergy H1, Hybrid Reader, Biotek Instruments, Winooski, VT, USA) at 570 nm with a 655-nm reference wavelength. In addition, the IC50 was calculated based on the MTT data.

Neutral Red This colorimetric analysis was performed to quantify membrane permeability and lysosomal cell activity in response to different doses of idebenone (0.06 and 0.03 µM). The protocol of this assay was previously described by Borenfreund and Puerner (1985). Briefy, primary muscle cells were washed in PBS once, and NR medium was added (250 µl), and the cells were incubated (37 °C) for 3 h. After this period, the NR medium was removed, the muscle cells were washed in PBS, and desorption solution was added. A shaker was used to extract the NR from the cells, and the absorbance was measured in a spectrophotometer (Synergy H1, Hybrid Reader, Biotek Instruments, Winooski, VT, USA) at 540 nm.

Intracellular calcium content

[Ca2+]i analysis was performed by Fluo-4 dye (Molecular Probes, Oregon, USA). The protocol was previously described (Macedo et al. 2015; Mizobuti et al. 2019). Briefly, after incubation with Fluo-4 AM, the calcium-sensitive dye intensities were observed on a fluorescent inverted microscope (Nikon, Eclipse TS100/TS100F) for qualitative data. Quantitative measurements were investigated using a spectrophotometer (Synergy H1, Hybrid Reader, Biotek Instruments, Winooski, VT, USA) at excitation and emission wavelengths of 494 and 516 nm, respectively.

H_2O_2 production

H_2O_2 levels were determined by Amplex® Red assay kit (Molecular Probes, Life Technologies, California, EUA) according to the manufacturer's instructions. The Amplex UltraRed reagent (50 µM) and HRP (0.1 U/ml) were added for 60 min. The absorbance was determined at 530- (excitation) and 590-nm wavelength (emission). Measurements of ROS were previously calibrated using exogenous 10 µM H_2O_2 (positive control). All measurements were performed in phenol red-free culture medium (1 ml), pH 7.4, at 37 °C.

Mitochondrial superoxide ($O2^{\bullet-}$) production

The mitochondrial superoxide ($O2^{\bullet-}$) production was determined by fluorescent dye MitoSOX™ Red (M36008, ThermoFisher) according to the manufacturer's instructions. Briefly, the dystrophic primary muscle cells were incubated with MitoSOX™ Red for 15 min at 37 °C. MitoSOX™ is selectively accumulated in the mitochondria, and it emits red fluorescence when oxidized by the superoxide anion.

The intensities of MitoSOX^{TM} fluorescence were monitored on a fluorescent inverted microscope (Nikon, Eclipse TS100/TS100F) for qualitative analyses. MitoSOX^{TM} Red was excited at 514 nm with the fluorescent images been collected at 570–600 nm. Quantitative measurements were performed using a spectrophotometer (Synergy H1, Hybrid Reader, Biotek Instruments, Winooski, VT, USA) at 510-nm excitation and 580-nm emission wavelengths.

Oxygen consumption

We evaluated oxygen consumption rates using an O2k-FluoRespirometer and used the DatLab software package (OROBOROS, Innsbruck, Austria) for data acquisition and analysis. After treatment, we trypsinized dystrophic muscle cells, centrifuged them (1250 RPM), and incubated them with 2 ml of air-saturated respiration medium in an Oxygraph-2k (O2k, OROBOROS Instruments). We used the following drugs in the assay: 1 µM oligomycin (Oligo), 2 µM carbonyl cyanate m-chlorophenyl hydrazone (CCCP), and 1 µM antimycin (Ant). We determined the basal oxygen consumption rate (OCR) by subtracting OCR pre-oligomycin from OCR post-antimycin; ATP-linked OCR was calculated by subtracting OCR post-oligomycin from OCR pre-oligomycin; proton leak was obtained by subtracting OCR post-oligomycin from OCR post-antimycin; maximal OCR was determined by subtracting OCR post-CCCP from OCR post-antimycin; reserve capacity was determined by subtracting OCR post-CCCP from OCR pre-oligomycin; and non-mitochondrial was the value of OCR post-antimycin.

Western blotting

The Western blotting protocol was previously described (Mizobuti et al. 2019; Rocha et al. 2022). Briefly, the Bradford method was used to determine the total protein content in cell extracts. Thirty micrograms of total protein homogenate was loaded on 6–15% SDS-polyacrylamide gels. After electrophoresis, the proteins were transferred onto nitrocellulose membranes, and the membranes were incubated with primary antibodies: 4-HNE (Bio-Rad AHP1251), Calpain 1 (Santa Cruz Biotechnology sc-7530), calsequestrin (Affinity BioReagents VIIID12), sarcolispin (Merckmilipore ABT 13), serca 2a (Cell-Sinaling 4388S), serca 1a (Cell-Sinaling D54G12), Oxphos (Abcam STN-19467), PGC-1α (Calbiochem 4C1.3), PPARδ (Invitrogen PA1-823A), SIRT-1 (Cell-Sinaling C14H4), and β-actin (Sigma-Aldrich A1978). Next, the membranes were incubated with the peroxidase-conjugated secondary antibodies: anti-rabbit (Promega Corporation W4011), anti-mouse (Promega Corporation W4021), and anti-goat (KPL14-13-06). To control protein loading, Western blot transfer, and nonspecific changes in protein levels, the blots were stripped and re-probed for β-actin. The ImageJ software was used to determine the band intensities.

Statistical analysis

All experiments were repeated independently at least three times. IC50 values of compounds were analyzed using GraphPad Prims 8 software package (GraphPad Software, CA, USA) using non-linear regression curve fitting with the normalized response. Statistical differences were analyzed using one-way ANOVA followed by Tukey test or Student's *t*-test using GraphPad Prism 8. Significant differences were defined as $P < 0.05$. All results are expressed as mean ± standard deviation (SD).

Results

Cell proliferation and viability

To assess the dose-dependent toxicities of idebenone on dystrophic muscle cells, we used the MTT and Neutral Red assays.

A significant reduction in cell proliferation in treated *mdx* muscle cells was observed in the MTT assay (Fig. 2A, B), when compared to untreated *mdx* muscle cells after 24-h treatment (93.0% for Ide 0.5 µM; 76.0% for Ide 0.25 µM; 42.4% for Ide 0.12 µM; 21.3% for Ide 0.06 µM; 93.0% for Ide 0.5 µM + LEDT; 81.6% for Ide 0.25 µM + LEDT; and 43.6% for Ide 0.12 µM + LEDT) and after 48-h treatment (93.7% for Ide 0.5 µM; 56.6% for Ide 0.25 µM; 21.5% for Ide 0.12 µM; 91.9% for Ide 0.5 µM + LEDT; and 67.0% for Ide 0.25 µM + LEDT).

The half maximal inhibitory concentrations (IC50) (Fig. 2C, D) at 24 h were 0.15 µM for idebenone and idebenone plus LEDT and at 48 h were 0.21 µM for idebenone and 0.20 µM idebenone plus LEDT.

Through the analysis of Neutral Red assay (Fig. 2E, F), a significant increase in the viability of treated *mdx* muscle cells was observed when compared to untreated mdx muscle cells after 24-h treatment (18.8% for Ide 0.06 µM; 15.3% for Ide 0.03 µM; 30.6% for LEDT; 22.6% for Ide 0.06 µM + LEDT; and 23.2% for Ide 0.03 µM + LEDT) and after 48-h treatment (23.6% for LEDT; 14.8% for Ide 0.06 µM + LEDT; and 22.7% for Ide 0.03 µM + LEDT).

Intracellular calcium content

Twenty-four hours after applying the treatments (idebenone, LEDT and/or idebenone plus LEDT), no significant

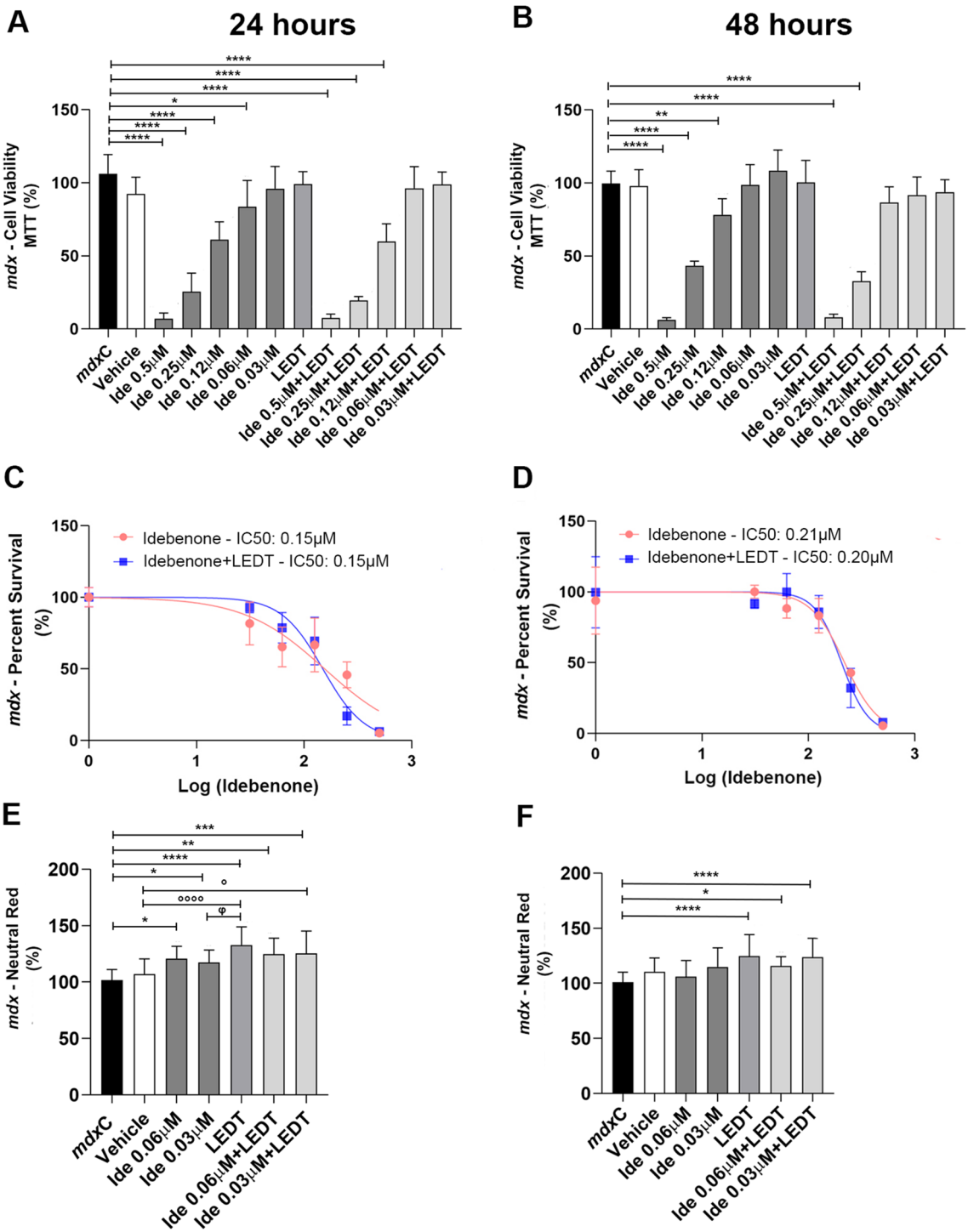

Fig. 2 MTT assay in untreated *mdx* muscle cells (*mdx*C); *mdx* muscle cells treated with carboxymethylcellulose sodium salt (Vehicle); *mdx* muscle cells treated with different doses of idebenone; *mdx* muscle cells treated with LEDT (LEDT); and *mdx* muscle cells treated with LEDT and different doses of idebenone, after 24 h (**A**) and 48 h (**B**). The half maximal inhibitory concentrations (IC50) in *mdx* muscle cells treated with different doses of idebenone and *mdx* muscle cells treated with LEDT and different doses of idebenone, after 24 h (**C**) and 48 h (**D**). Neutral Red assay in *mdx*C; vehicle; *mdx* muscle cells treated with 0.06 μM and 0.03μM of idebenone, LEDT, and LEDT and 0.06μM and 0.03μM of idebenone, after 24 h (**E**) and 48 h (**F**). All data are expressed by mean ± SD, and the experiments were carried out in triplicate. $^{*}P < 0.05$ versus *mdx*C; $^{**}P < 0.01$ versus *mdx*C; $^{***}P < 0.001$ versus *mdx*C; $^{****}P < 0.00001$ versus *mdx*C; $^{\circ}P < 0.05$ versus vehicle; $^{\circ\circ\circ\circ}P < 0.00001$ versus vehicle; $^{\varphi}P < 0.05$ versus Ide 0.03 μM

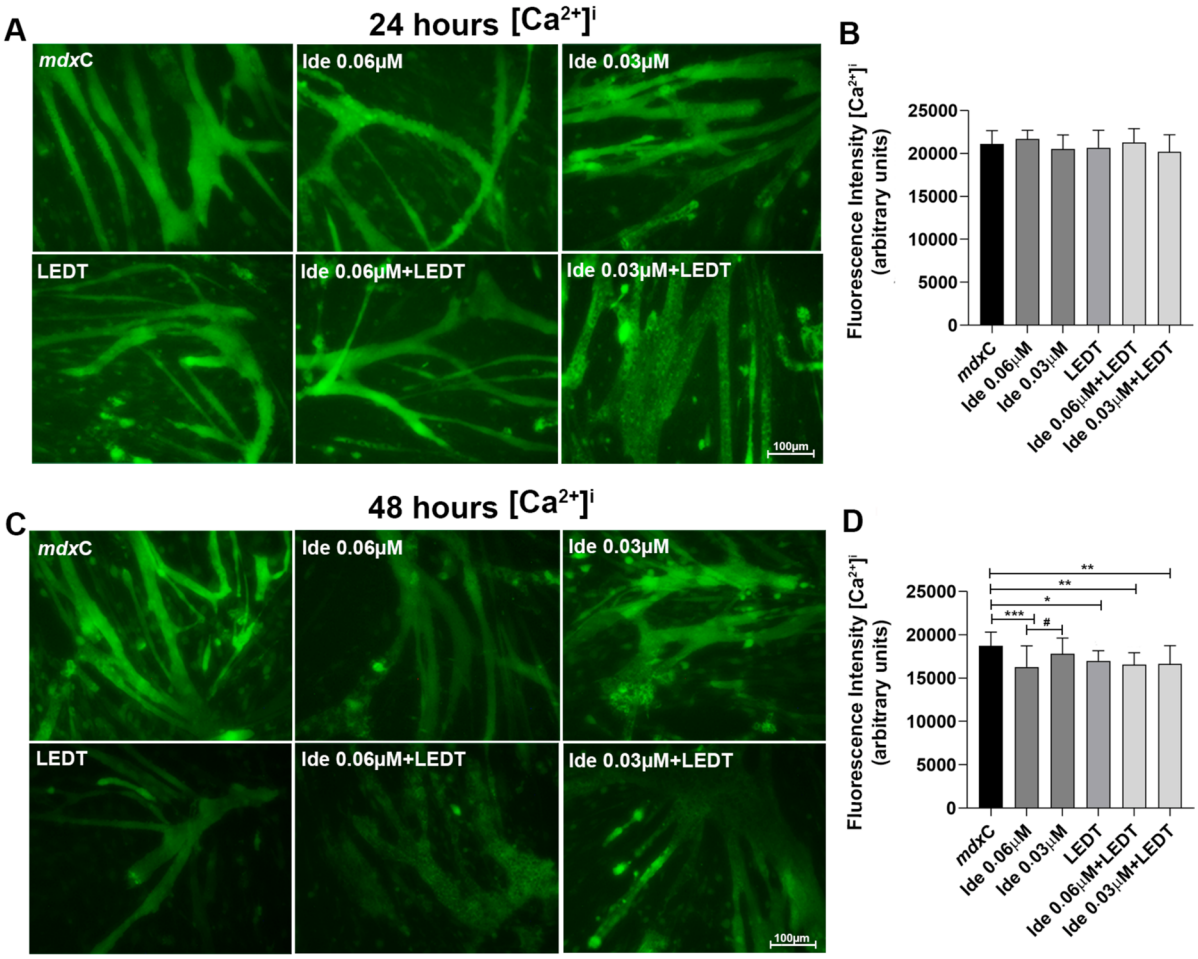

Fig. 3 Intracellular calcium concentrations [Ca2+]i in untreated *mdx* muscle cells (*mdx*C); *mdx* muscle cells treated with 0.06 μM and 0.03 μM of idebenone; *mdx* muscle cells treated with LEDT; and *mdx* muscle cells treated with LEDT and 0.06 μM and 0.03 μM of idebenone, after 24 h (**A**) and 48 h (**C**). Scale bar: 100 μm, × 20. Graph showing fluorescence intensity of [Ca2+] in experimental groups, after 24 h (**B**) and 48 h (**D**) of LEDT and idebenone treatment. All data are expressed by mean ± SD, and the experiments were carried out in triplicate. $^{*}P < 0.05$ versus *mdx*C; $^{**}P < 0.01$ versus *mdx*C; $^{***}P < 0.001$ versus *mdx*C; $^{\#}P < 0.05$ versus Ide 0.06 μM

difference in [Ca2+]i was observed between the experimental groups (Fig. 3A, B). On the other hand, 48 h after treatments, the treated-*mdx* muscle cells showed a significant reduction of [Ca2+]i (13.0% for Ide 0.06 μM; 9.1% for LEDT; 11.6% for Ide 0.06 μM + LEDT; and 11.0% for Ide 0.03 μM + LEDT) compared to the untreated *mdx* muscle cells (Fig. 3C, D).

Oxidative stress

Twenty-four hours after applying the treatments (idebenone, LEDT and/or idebenone plus LEDT), the treated-*mdx* muscle cells showed a significant reduction of $O_2^{\bullet-}$ production (16.6% for Ide 0.06 μM; 15.6% for Ide 0.03 μM; 12.1% for LEDT; 13.6% for Ide 0.06 μM + LEDT; and 12.0% for Ide 0.03 μM + LEDT) compared to the untreated *mdx* muscle cells (Fig. 4A, B). Similar results were also observed after 48 h of treatments (14.7% for Ide 0.06 μM; 15.1% for Ide 0.03 μM; 19.3% for LEDT; 15.3% for Ide 0.06 μM + LEDT; and 12.8% for Ide 0.03 μM + LEDT) compared to the untreated *mdx* muscle cells (Fig. 4D, E).

Regarding H_2O_2 production, the treated-*mdx* muscle cells analyzed 24 h after all the treatments showed a significant reduction in its production (12.6% for Ide 0.06 μM; 12.9% for Ide 0.03 μM; 10.9% for LEDT; 18.0% for Ide 0.06 μM + LEDT; and 14.3% for Ide 0.03 μM + LEDT) compared to the untreated *mdx* muscle cells (Fig. 4C). However, 48 h after the treatments, only *mdx* muscle cells treated with Ide 0.06 μM, LEDT, and Ide 0.06 μM + LEDT showed a significant reduction in H_2O_2 production (by 16.0%, 8.9%, and 13.0%, respectively) compared to the untreated *mdx* muscle cells (Fig. 4F).

Regarding the lipidic peroxidation marker, the *mdx* muscle cells treated with Ide 0.06 μM, LEDT, and Ide 0.06μM +

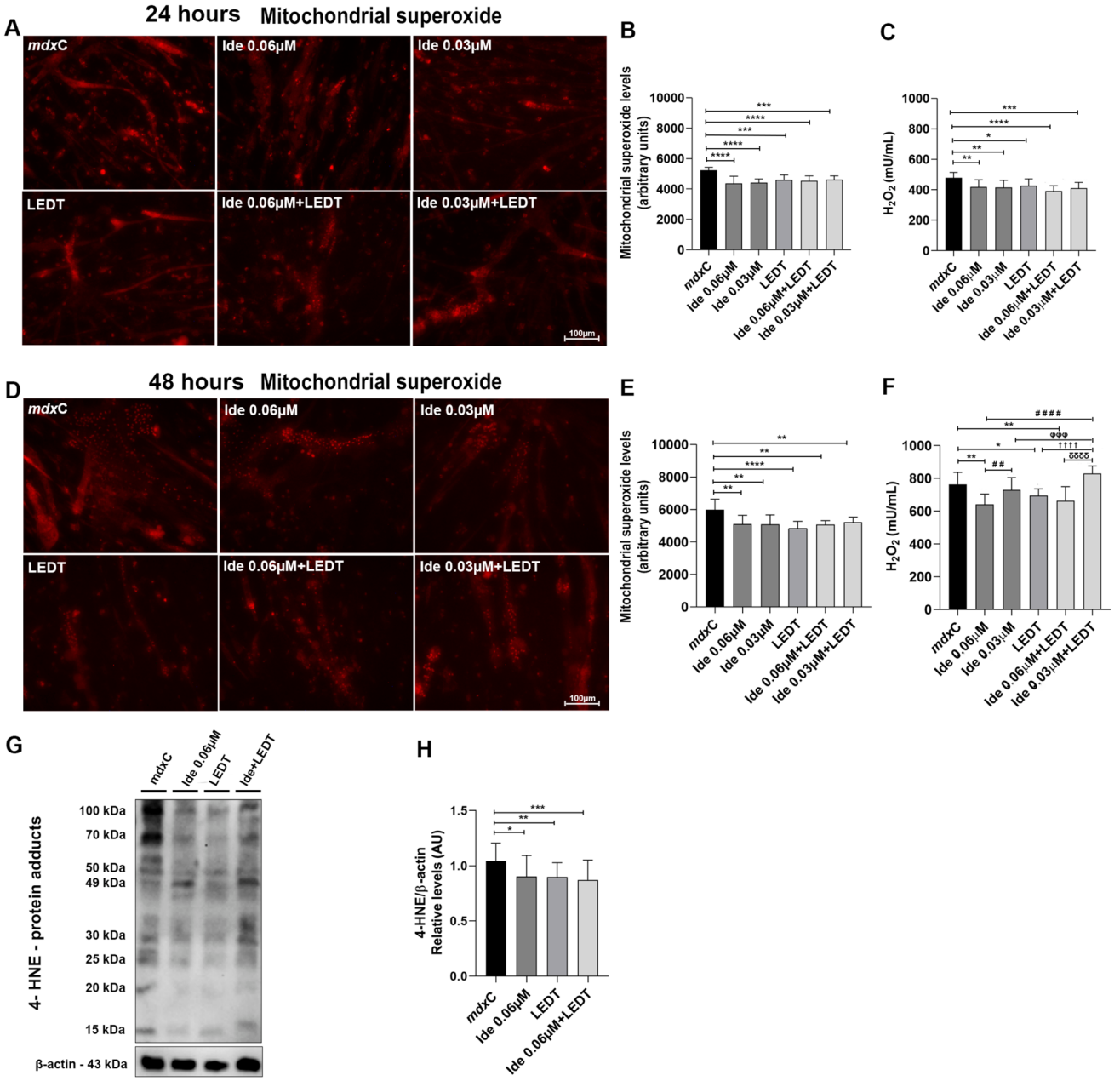

Fig. 4 MitoSOX^{TM} fluorescence (red) images in untreated *mdx* muscle cells (*mdx*C); *mdx* muscle cells treated with 0.06 μM and 0.03 μM of idebenone; *mdx* muscle cells treated with LEDT; and *mdx* muscle cells treated with LEDT and 0.06 μM and 0.03 μM of idebenone, after 24 h (**A**) and 48 h (**D**). Scale bar 100 μm, × 20. Graphs showing MitoSOX^{TM} fluorescence intensity in experimental groups, after 24 h (**B**) and 48 h (**E**) of LEDT and idebenone treatments. The graphs show H_2O_2 production in experimental groups, after 24 h (**C**) and 48 h (**F**) of LEDT and idebenone treatments. Western blotting analysis of 4-HNE protein adducts (**G**) in *mdx*C; *mdx* muscle cells treated with 0.06 μM of idebenone; LEDT; and *mdx* muscle cells treated with LEDT and 0.06 μM of idebenone. The graphs (**H**) show 4-HNE protein adducts levels in experimental groups. β-Actin was used as a loading control. The relative value of the band intensity was quantified and normalized by the corresponding control. All data are expressed by mean ± SD, and the experiments were carried out in triplicate. $^{*}P < 0.05$ versus *mdx*C; $^{**}P < 0.01$ versus *mdx*C; $^{***}P < 0.001$ versus *mdx*C; $^{****}P < 0.00001$ versus *mdx*C; $^{\#\#}P < 0.01$ versus Ide 0.06 μM; $^{\#\#\#\#}P < 0.00001$ versus Ide 0.06 μM; $^{\varphi\varphi\varphi}P < 0.001$ versus Ide 0.03 μM; $^{\dagger\dagger\dagger\dagger}P < 0.00001$ versus LEDT; $^{\delta\delta\delta\delta}P < 0.00001$ versus Ide 0.06 μM+LEDT

LEDT (analyzed 48 h after treatments) showed a significant reduction in 4-HNE protein adduct levels (by 10.0%, 11.0%, and 13%, respectively) compared to the untreated *mdx* muscle cells (Fig. 4G, H).

Calcium pathways

Regarding calpain-1, the *mdx* muscle cells treated with Ide 0.06 µM, LEDT, and Ide 0.06 µM + LEDT showed a significant reduction in its levels (by 57.7%, 46.2%, and 64.7%, respectively) compared to the untreated *mdx* muscle cells (Fig. 5A, B).

The calsequestrin levels were significantly reduced in the *mdx* muscle cells treated with LEDT and Ide 0.06 µM + LEDT (by 83.0% and 80.9%%, respectively) compared to the untreated *mdx* muscle cells (Fig. 5A, B).

In relation to sarcolispin and serca 2a levels, only the *mdx* muscle cells treated with Ide 0.06µM + LEDT showed a significant reduction in their levels (by 49.2% and 30.0%, respectively) compared to the untreated *mdx* muscle cells (Fig. 5A, B).

The serca 1a levels were significantly increased in the *mdx* muscle cells treated with Ide 0.06 µM, LEDT, and Ide 0.06 µM + LEDT (by 227.4%, 201.9%, and 205.8%, respectively) compared to the untreated *mdx* muscle cells (Fig. 5A, B).

Mitochondrial pathways

The OCR was evaluated, and it was found that the *mdx* muscle cells treated with Ide 0.06 µM increased the basal, ATP-linked, and maximal capacity (by 98.8%, 100.0%, and 55.2%, respectively) compared to the *mdx* untreated muscle cells (Fig. 6A). In addition, the basal, ATP-linked, maximal and spare capacity were increased in the *mdx* muscle cells treated with LEDT (by 107.8%, 201.5%, 138.7%, and 511.7%, respectively) and/or Ide 0.06 µM + LEDT (by 51.8%, 85.8%, 96.9%, and 198.6%, respectively) compared to the untreated *mdx* muscle cells (Fig. 6A).

The *mdx* muscle cells treated with Ide 0.06 µM, LEDT, and Ide 0.06 µM + LEDT presented a significant increase in the OXPHOS levels in complex V (by 125.0%, 94.1%, and 182.3%, respectively) compared to the untreated *mdx* muscle cells (Fig. 6B, C). In addition, the *mdx* muscle cells treated with Ide 0.06µM + LEDT, also showed a significant increase in complex II and I (by 39.1% and 55.4%, respectively) compared to the untreated *mdx* muscle cells (Fig. 6B, C).

Regarding PGC-1α, the *mdx* muscle cells treated with Ide 0.06 µM, LEDT, and Ide 0.06µM + LEDT presented a significant increase in its levels (by 27.0%, 32.8%, and 27.0%, respectively) compared to the untreated *mdx* muscle cells (Fig. 6D, E). Similar results were also observed in PPARδ where the *mdx* muscle cells treated with Ide 0.06µM, LEDT, and Ide 0.06µM + LEDT presented a significant increase in its levels (by 66.6%, 33.3%, and 38.8%, respectively) compared to the untreated *mdx* muscle cells (Fig. 6D, E).

On the other hand, only the *mdx* muscle cells treated with Ide 0.06 µM + LEDT showed a significant increase in SIRT-1 levels (31.8%), compared to the untreated *mdx* muscle cells (Fig. 6D, E).

Discussion

Here, we demonstrated beneficial effects in calcium and mitochondrial signaling pathways in dystrophic muscle cells subjected to LEDT and idebenone treatment applied separately and/or together.

Although the mechanisms involved in DMD are complex and multifactorial, impaired calcium handling and calcium overload are key contributors to disease onset and progression (Mareedu et al. 2021). Increased intracellular

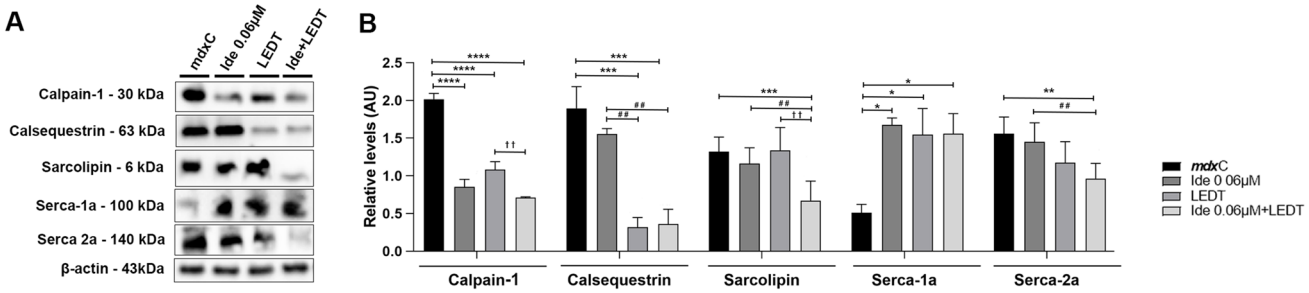

Fig. 5 **A** Western blotting analysis of calpain-1, calsequestrin, sarcolipin, serca-1a, serca-2a in untreated *mdx* muscle cells (*mdx*C); *mdx* muscle cells treated with 0.06 µM of idebenone; *mdx* muscle cells treated with LEDT; and *mdx* muscle cells treated with LEDT and 0.06 µM of idebenone. **B** The graph shows the protein levels. β-Actin was used as an internal control. The relative value of the band intensity was quantified and normalized by the corresponding control. All data are expressed by mean ± SD, and the experiments were carried out in triplicate. $^{*}P < 0.05$ versus *mdx*C; $^{**}P < 0.01$ versus *mdx*C; $^{***}P < 0.001$ versus *mdx*C; $^{****}P < 0.00001$ versus *mdx*C; $^{\#\#}P < 0.01$ versus Ide 0.06 µM; $^{\dagger\dagger}P < 0.05$ versus LEDT

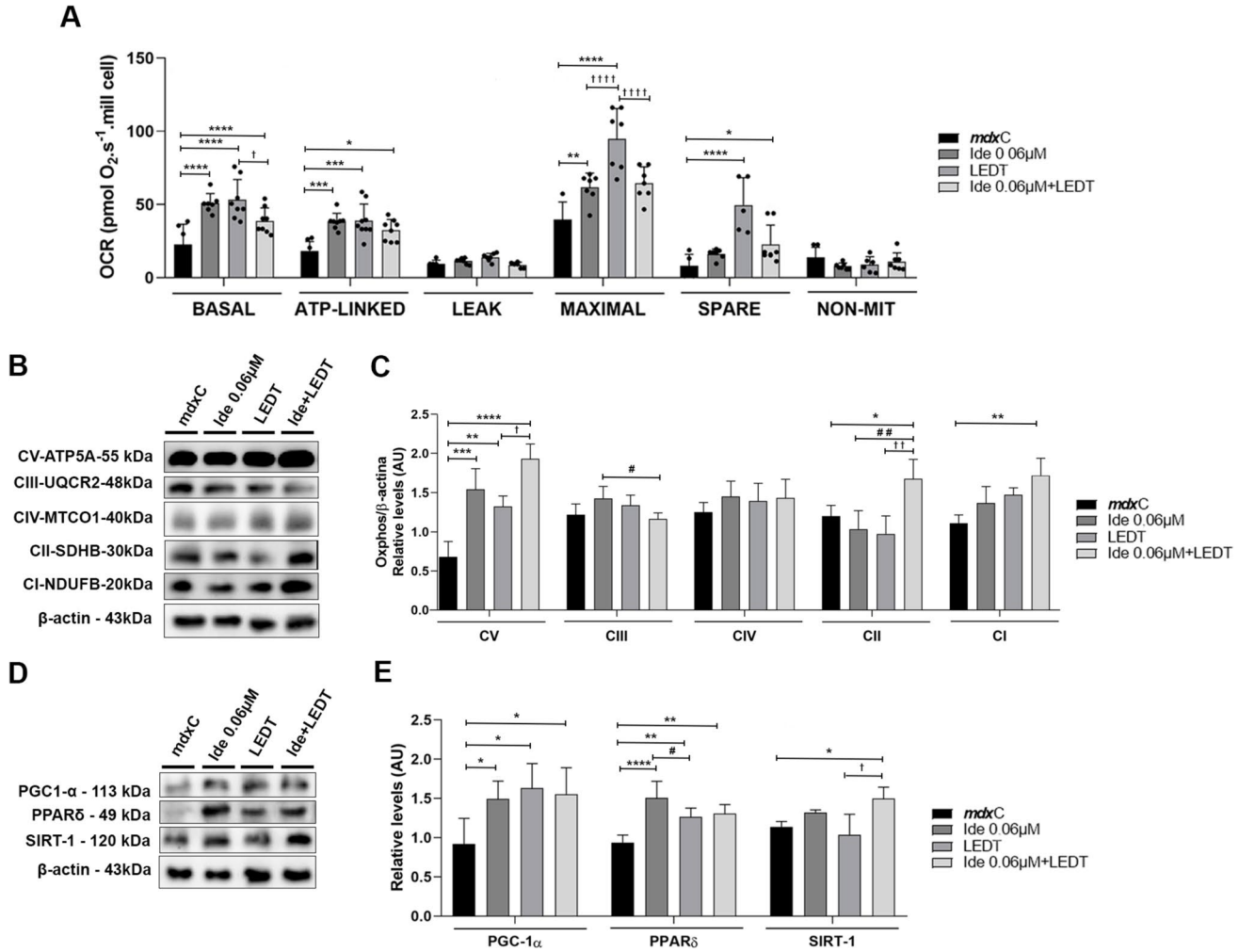

Fig. 6 **A** OCR values were measured in untreated *mdx* muscle cells (*mdx*C), *mdx* muscle cells treated with 0.06 µM of idebenone, *mdx* muscle cells treated with LEDT, and *mdx* muscle cells treated with LEDT and 0.06 µM of idebenone. The measurements were taken for basal, ATP-linked, leak, maximal, and spare capacity. Non-mitochondrial OCR was subtracted from all data before being used for these analyses. **B** Western blotting analysis of OXPHOS and **D** of PGC-1α, PPARδ, and SIRT-1in untreated *mdx* muscle cells (*mdx*C); *mdx* muscle cells treated with 0.06 µM of idebenone; *mdx* muscle cells treated with LEDT; and *mdx* muscle cells treated with LEDT and 0.06 µM of idebenone. **C**, **E** The graph shows the protein levels. β-Actin was used as an internal control. The relative value of the band intensity was quantified and normalized by the corresponding control. All data are expressed by mean ± SD, and the experiments were carried out in triplicate. $^{*}P < 0.05$ versus *mdx*C; $^{**}P < 0.01$ versus *mdx*C; $^{***}P < 0.001$ versus *mdx*C; $^{****}P < 0.00001$ versus *mdx*C; $^{\#}P < 0.05$ versus Ide 0.06 µM; $^{\#\#}P < 0.01$ versus Ide 0.06 µM; $^{\dagger}P < 0.05$ versus LEDT; $^{\dagger\dagger}P < 0.01$ versus LEDT; $^{\dagger\dagger\dagger\dagger}P < 0.00001$ versus LEDT

calcium in the context of dystrophin deficiency is a main mediator in myocyte death and fibrotic development (Shirokova et al. 2013). Under our experimental conditions, we observed that LEDT and idebenone treatment decreased the $[Ca^{2+}]_i$ in *mdx* muscle cells. Concomitant with the decrease in $[Ca^{2+}]_i$, a significant finding of this study was the decrease in sarcolipin (SLN) levels. In agreement with our results, a previous study found improvement in the cytosolic Ca^{2+} homeostasis in *mdx* mice lacking SLN (Tanihata et al. 2018).

SLN is an important regulator of the SERCA pump, which is expressed exclusively in the striated muscle of all mammals (Vangheluwe et al. 2005). A previous study provides evidence that SLN upregulation is a molecular basis for SERCA dysfunction in both DMD skeletal and cardiac muscles (Voit et al. 2017). In addition, SLN knockout mice display an increase in the SERCA function (Tupling et al. 2011; Bombardier et al. 2013). Enhancing the SERCA expression or activity appears to be a promising strategy to treat the dystrophic skeletal muscle, since SERCA accounts for ≥ 70% of Ca2+ removal from the cytosol (Periasamy and Kalyanasundaram 2007; Tupling 2009). It is important to note that in the present study, we also showed an increase in SERCA 1 levels, which is the primary isoform express in the fast-twitch skeletal muscle (Wu and Lytton 1993). However, we also found a reduction in the SERCA 2 levels. In the skeletal muscle, there are some inhibitory proteins that alter

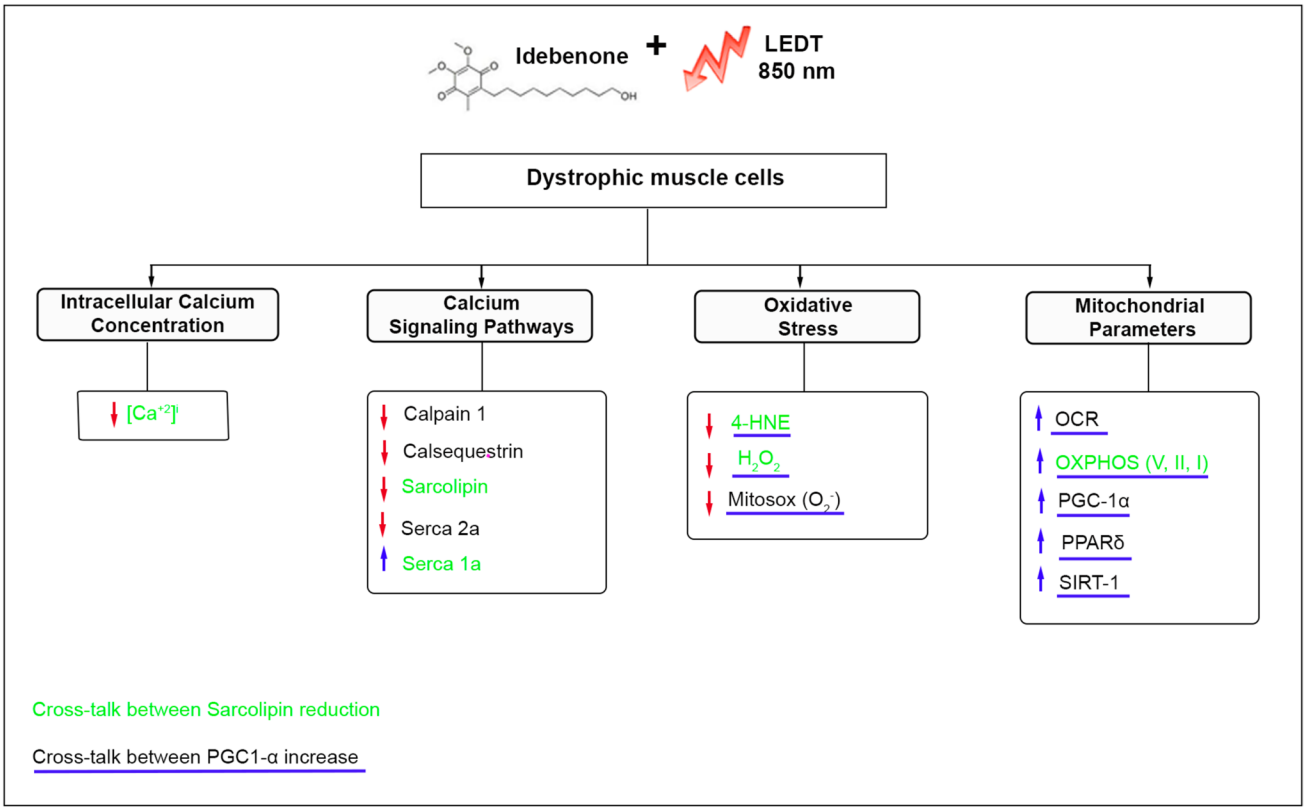

Fig. 7 LEDT and idebenone treatment effects on mdx muscle cells. Upregulation: blue up arrow; downregulation: red down arrow; cross-talk between sarcolipin reduction: words in green; cross-talk between PGC1-α increase: word underlined in blue

the SERCA action, such as SLN (as mentioned before) and phospholamban (PLN) (Gamu et al. 2020). In vivo studies have consistently found that PLN preferentially binds with SERCA 2, which is highly expressed in the cardiac and slow-twitch muscle (Fujii et al. 1988; Briggs et al. 1992; Babu et al. 2007; Fajardo et al. 2013). On the other hand, SLN has been associated to SERCA 1 (Maclennan et al. 1973). Thus, these previous studies can collaborate with our findings about SERCA and SLN.

Still regarding the calcium signaling pathways, we found a reduction in the levels of calpain-1 and calsequestrin after LEDT and idebenone treatment. It is already well established that the increase in $[Ca^{2+}]_i$ could activate calpains, thereby promoting muscle wasting through increased proteolysis in dystrophic muscles (Bodensteiner and Engel 1978; Spencer et al. 1995). In addition, it was reported that isolated *mdx* muscle fibers exhibit heightened calpain-mediated proteolysis when compared with normal muscle fibers (Gailly et al. 2007). Thus, targeting a reduction in calpain levels is a promising approach in DMD treatment. On the other hand, calsequestrin (the most abundant calcium-binding protein) showed higher levels in the spared muscles of *mdx* mice (Pertille et al. 2010). However, in our experimental conditions, we observed a reduction in calsequestrin levels, suggesting that the decrease of $[Ca^{2+}]_i$, by other pathways, after LEDT and idebenone treatment, reduced the need for its upregulation.

Another potential target related to impaired Ca^{2+} homeostasis in dystrophic muscles is the mitochondria (Robert et al. 2001). Reduced mitochondrial respiration and increased calcium deposits were reported in the fast-twitch muscle fibers of *mdx* mice (Gaglianone et al. 2019). In addition, mitochondrial Ca^{2+} overload can cause mitochondrial ROS production contributing to oxidative stress in dystrophic muscles (Kyrychenko et al. 2015). In the present study, using LEDT and idebenone treatment, we observed improved oxidative capacity in dystrophic muscle cells, by OCR and OXPHOS analyzes. Concomitantly, we also found reduced levels of ROS and lipid peroxidation after treatment. A main mechanism of the beneficial effect of LEDT relies on the improvement of the mitochondrial function by the direct stimulation of the electron transfer chain (Salechpour et al. 2018b). Several studies showed that PBMT can improve mitochondrial functions by increasing ATP and the mitochondrial membrane potential and by decreasing ROS production (Salechpour et al. 2017, 2018a, 2018b). Regarding idebenone, its ability to modulate

the activity of the mitochondrial respiratory chain complexes, as well as its capacity to protect membranes against lipid peroxidation, is well known (Muscoli et al. 2002).

It is also important to highlight that the reduction in SLN levels correlates with the interplay between mitochondrial function and oxidative stress. Supporting what was said before, the reduction of SLN restored the complex proteins (OXPHOS) and their activities, as well as reducing the protein carbonyl content and lipid peroxidation, thus indicating reduced oxidative stress in the dystrophic muscles (Balakrishnan et al. 2022). Interestingly, in the present study, we also observed a reduction in SLN levels in the dystrophic muscle cells treated, suggesting that this signaling pathway may also be one of the mechanisms by which the LEDT and idebenone treatment showed antioxidant effects and improved mitochondrial function in the dystrophic muscle.

The signaling pathway between the silent mating type information regulation 2 homolog 1 (SIRT1), peroxisome proliferator-activated receptor (PPARs), and peroxisome proliferator-activated receptor-γ coactivator-1α (PGC-1α) could be another possible explanation for observed ROS reduction in the dystrophic muscle cells. PGC-1α is a main regulator of mitochondrial biogenesis and function in several tissues (Handschin and Spiegelman 2006) and is regulated by PPARs and SIRT1 (Cantó and Auwerx 2009). LEDT and idebenone treatment increased SIRT1, PPARδ, and PGC-1α in the dystrophic muscle cells, in our study. In agreement with our results, previous studies have demonstrated that PBMT can induce mitochondrial biogenesis by the elevation of SIRT1 and PGC-1α in the C_2C_{12} muscle cells (Nguyen et al. 2014) and in a transient cerebral ischemia mouse model (Salehpour et al. 2019). Recently, our research group also reported the correlation between elevated PGC-1α levels and oxidative stress reduction in the dystrophic muscle treated with antioxidants (Silva et al. 2021; Mizobuti et al. 2022). Regarding idebenone, a previous study, collaborating with our results, showed that this antioxidant can positively influence mitochondrial biogenesis by increasing PPARGC1A gene expression in human-induced pluripotent stem cells (Augustyniak et al. 2017).

However, despite the novelty of this study, one limitation must be recognized. While the beneficial effects reported after LEDT and idebenone treatment are statistically significant, the relative change when compared to the control group is low. This fact may have occurred because a single application of LEDT and only one dose of antioxidant were evaluated. In addition, the analysis period after the treatments may also have interfered with the results obtained. In view of this, we intend to evaluate new variables (e.g., several LEDT applications and different exposure periods to the antioxidant treatment) in future experiments.

Summarizing, our findings suggest that LEDT and idebenone treatment, alone or together, can modulate the calcium and mitochondrial signaling pathways, such as SLN, SERCA 1, and PGC-1α, contributing to the improvement of the dystrophic phenotype in muscle cells (Fig. 7). It is also important to highlight that data from the LEDT plus idebenone treatment showed slightly better results than those of each separate treatment in terms of SLN, OXPHOS, and SIRT-1. In addition, this work contributes to the knowledge that the combining of new approaches holds promise for better and more specific DMD treatments in the future. The combined therapies usually show a synergistic effect and act on the treatment of the secondary consequences of the muscular dystrophy (e.g., oxidative stress and mitochondrial dysfunction) and are more effective than single therapies. Therefore, the future technical advances in combined therapeutic assays will help to lead to more effective treatment for DMD.

Acknowledgements We thank Mrs. Deirdre Jane Donovan Giraldo for the English revision of the manuscript.

Funding This research was funded by Fundação de Amparo à Pesquisa do Estado de São Paulo (FAPESP; #2020/09733-4), Coordenação de Pessoal de Nível Superior-Brasil (CAPES)–Finance Code 001, CNPq, and FAEPEX. G.L.R. and D.S.M. were the recipients of a CAPES fellowship. H.N.M.S., V.A.P., E.M., and M.V.C. are the recipients of a CNPq fellowship. A.G.O. received a scholarship from FAPESP (# 2018/20581-1).

Declarations

Conflict of interest The authors declare no competing interests.

References

Augustyniak J, Lenart J, Zychowicz M, Stepien PP, Buzanska L (2017) Mitochondrial biogenesis and neural differentiation of human iPSC is modulated by idebenone in a developmental stage-dependent manner. Biogerontology 18:665–677. https://doi.org/10.1007/s10522-017-9718-4

Babu GJ, Bhupathy P, Carnes CA, Billman GE, Periasamy M (2007) Differential expression of sarcolipin protein during muscle development and cardiac pathophysiology. J Mol Cell Cardiol 43:215–222. https://doi.org/10.1016/j.yjmcc.2007.05.009

Balakrishnan R, Mareedu S, Babu GJ (2022) Reducing sarcolipin expression improves muscle metabolism in *mdx* mice. Am J Physiol Cell Physiol 322:C260–C274. https://doi.org/10.1152/ajpcell.00125.2021

Bodensteiner JB, Engel AG (1978) Intracellular calcium accumulation in Duchenne dystrophy and other myopathies: a study of 567,000 muscle fibers in 114 biopsies. Neurology 28:439–446. https://doi.org/10.1212/wnl.28.5.439

Bombardier E, Smith IC, Vigna C, Fajardo VA, Tupling AR (2013) Ablation of sarcolipin decreases the energy requirements for Ca2 þ transport by sarco(endo)plasmic reticulum Ca2 þ -ATPases in resting skeletal muscle. FEBS Lett 587:1687–1692. https://doi.org/10.1016/j.febslet.2013.04.019

Borenfreund E, Puerner JA (1985) Toxicity determined in vitro by morphological alterations and neutral red absorption. Toxicol Lett. 24(2–3):119–24. https://doi.org/10.1016/0378-4274(85)90046-3

Briggs FN, Lee KF, Wechsler AW, Jones LR (1992) Phospholamban expressed in slow-twitch and chronically stimulated fast-twitch muscles minimally affects calcium affinity of sarcoplasmic reticulum Ca(2þ)-ATPase. J Biol Chem 267:26056–26061. https://doi.org/10.1016/S0021-9258(18)35716-8

Buyse GM, Gueven N, McDonald CM (2015) Idebenone as a novel therapeutic approach for Duchenne muscular dystrophy. Eur Neurol Rev 10:189–194. https://doi.org/10.17925/ENR.2015.10.02.189

Cantó C, Auwerx J (2009) PGC-1alpha, SIRT1 and AMPK, an energy sensing network that controls energy expenditure. Curr Opin Lipidol 20:98–95. https://doi.org/10.1097/MOL.0b013e328328d0a4

Emery AEH (2002) The muscular dystrophies. Lancet 359:687–695. https://doi.org/10.1016/S0140-6736(02)07815-7

Fajardo VA, Bombardier E, Vigna C, Devji T, Bloemberg D, Gamu D, Gramolini AO, Quadrilatero J, Tupling AR (2013) Co-expression of SERCA isoforms, phospholamban and sarcolipin in human skeletal muscle fibers. PloS One 8:e84304. https://doi.org/10.1371/journal.pone.0084304

Freitas LF, Hamblin MR (2016) Proposed mechanisms of photobiomodulation or low-level light therapy. IEEE J Sel Top Quantum Electron 22:7000417. https://doi.org/10.1109/JSTQE.2016.2561201

Fujii J, Lytton J, Tada M, MacLennan DH (1988) Rabbit cardiac and slow-twitch muscle express the same phospholamban gene. FEBS Lett 227:51–55. https://doi.org/10.1016/0014-5793(88)81412-1

Gaglianone RB, Santos AT, Bloise FF, Ortiga-Carvalho TM, Costa ML, Quirico-Santos T, da Silva WS, Mermelstein C (2019) Reduced mitochondrial respiration and increased calcium deposits in the EDL muscle, but not in soleus, from 12-week-old dystrophic *mdx* mice. Sci Rep 9:1986. https://doi.org/10.1038/s41598-019-38609-4

Gailly P, De Backer F, Van Schoor M, Gillis JM (2007) In situ measurements of calpain activity in isolated muscle fibres from normal and dystrophin-lacking mdx mice. J Physiol 582:1261–1275. https://doi.org/10.1113/jphysiol.2007.132191

Gamu D, Juracic ES, Hall KJ, Tupling AR (2020) The sarcoplasmic reticulum and SERCA: a nexus for muscular adaptive thermogenesis. Appl Physiol Nutr Metab 45:1–10. https://doi.org/10.1139/apnm-2019-0067

Gloss D, Moxley RT 3rd, Ashwal S, Oskoui M (2016) Practice guideline update summary: corticosteroid treatment of Duchenne muscular dystrophy: report of the Guideline Development Subcommittee of the American Academy of Neurology. Neurology 86:465–472. https://doi.org/10.1212/WNL.0000000000002337

González-Jamett A, Vásquez W, Cifuentes-Riveros G, Martínez-Pando R, Sáez JC, Cárdenas AM (2022) Oxidative stress, inflammation and connexin hemichannels in muscular dystrophies. Biomedicines 10:507. https://doi.org/10.3390/biomedicines10020507

Handschin C, Spiegelman BM (2006) Peroxisome proliferator-activated receptor gamma coactivator 1 coactivators, energy homeostasis, and metabolism. Endocr Rev 27:728–735. https://doi.org/10.1210/er.2002-0012

Hussain T, Mangath H, Sundaram C, Anandaraj MPJS (2000) Expression of the gene for large subunit of m-calpain is elevated in skeletal muscle from Duchenne muscular dystrophy patients. J Genet 79:77–80. https://doi.org/10.1007/Bf02728949

Karu TI (2008) Mitochondrial signaling in mammalian cells activated by red and near-IR radiation. Photochem Photobiol 84:1091–1099. https://doi.org/10.1111/j.1751-1097.2008.00394.x

Kyrychenko V, Poláková E, Janícek R, Shirokova N (2015) Mitochondrial dysfunctions during progression of dystrophic cardiomyopathy. Cell Calcium 58:186–195. https://doi.org/10.1016/j.ceca.2015.04.006

Landfeldt E, Edström J, Buccella F, Kirschner J, Lochmüller H (2018) Duchenne muscular dystrophy and caregiver burden: a systematic review. Dev Med Child Neurol 60:987–996. https://doi.org/10.1111/dmcn.13934

Macedo AB, Mizobuti DS, Hermes TA, Mancio RD, Pertille A, Kido LA, Cagnon VHA, Minatel E (2020) Photobiomodulation therapy for attenuating the dystrophic phenotype of Mdx mice. Photochem Photobiol 96:200–207. https://doi.org/10.1111/php.13179

Macedo AB, Moraes LHR, Mizobuti DS, Fogaca AR, Moraes FRS, Hermes TA, Pertille A, Minatel E (2015) Low-level laser therapy (LLLT) in dystrophin-deficient muscle cells: effects on regeneration capacity, inflammation response and oxidative stress. PloS One 10:e0128567. https://doi.org/10.1371/journal.pone.0128567

Maclennan DH, Yip CC, Iles GH, Seeman P (1973) Isolation of sarcoplasmic reticulum proteins. Cold Spring Harb Sym 37:469–477. https://doi.org/10.1101/SQB.1973.037.01.058

Mareedu S, Million ED, Duan D, Babu GJ (2021) Abnormal calcium handling in Duchenne muscular dystrophy: mechanisms and potential therapies. Front Physiol 12:647010. https://doi.org/10.3389/fphys.2021.647010

Mizobuti DS, Fogaca AR, Moraes FRS, Moraes LHR, Mancio RD, Hermes TA, Macedo AB, Valduga AH, Lourenco CC, Pereira ECL, Minatel E (2019) Coenzyme Q10 supplementation acts as antioxidant on dystrophic muscle cells. Cell Stress Chaperones 24:1175–1185. https://doi.org/10.1007/s12192-019-01039-2

Mizobuti DS, Rocha GL, Silva HNM, Covatti C, Lourenço CC, Pereira ECL, Salvador MJ, Minatel E (2022) Antioxidant effects of bisindole alkaloid indigo and related signaling pathways in the experimental model of Duchenne muscular dystrophy. Cell Stress Chaperones 27:417–429. https://doi.org/10.1007/s12192-022-01282-0

Moore TM, Lin AJ, Strumwasser AR, Cory K, Whitney K, Ho T, Ho T, Lee JL, Rucker DH, Nguyen CQ, Yackly A, Mahata SK, Wanagat J, Stiles L, Turcotte LP, Crosbie RH, Zhou Z (2020) Mitochondrial dysfunction is an early consequence of partial or complete dystrophin loss in mdx mice. Front Physiol 11:690. https://doi.org/10.3389/fphys.2020.00690

Moxley RT 3rd, Pandya S, Ciafaloni E, Fox DJ, Campbell K (2010) Change in natural history of Duchenne muscular dystrophy with long-term corticosteroid treatment: Implications for Management. J Child Neurol 25(9):1116–1129. https://doi.org/10.1177/0883073810371004

Muscoli C, Fresta M, Cardile V, Palumbo M, Renis M, Puglisi G, Paolino D, Nisticò S, Rotiroti D, Mollace V (2002) Ethanol-induced injury in rat primary cortical astrocytes involves oxidative stress: effect of idebenone. Neurosci Lett 329:21–24. https://doi.org/10.1016/s0304-3940(02)00567-0

Nguyen LM, Malamo AG, Larkin-Kaiser KA, Borsa PA, Adhihetty PJ (2014) Effect of near-infrared light exposure on mitochondrial signaling in C 2 C 12 muscle cells. Mitochondrion 14:42–48. https://doi.org/10.1016/j.mito.2013.11.001

Periasamy M, Kalyanasundaram A (2007) SERCA pump isoforms: their role in calcium transport and disease. Muscle Nerve 35:430–442. https://doi.org/10.1002/mus.20745

Pertille A, Carvalho CLT, Matsumura CY, Neto HS, Marques MJ (2010) Calcium-binding proteins in skeletal muscles of the mdx mice: potential role in the pathogenesis of Duchenne muscular dystrophy. Int J Exp Pathol 91:63–71. https://doi.org/10.1111/j.1365-2613.2009.00688.x

Rando TA, Blau HM (1994) Primary mouse myoblast purification, characterization, and transplantation for cell-mediated gene therapy. J Cell Biol 125:1275–1287. https://doi.org/10.1083/jcb.125.6.1275

Robert V, Massimino ML, Tosello V, Marsault R, Cantini M, Sorrentino V, Pozzan T (2001) Alteration in calcium handling at the subcellular level in mdx myotubes. J Biol Chem 276:4647–4651. https://doi.org/10.1074/jbc.M006337200

Rocha GL, Mizobuti DS, Silva HNM, Covatti C, Lourenço CC, Salvador MJ, Pereira EL, Minatel E (2022) Multiple LEDT wavelengths modulate the Akt signaling pathways and attenuate pathological events in mdx dystrophic muscle cells. Photochem Photobiol Sci 21:1257–1272. https://doi.org/10.1007/s43630-022-00216-0

Salehpour F, Ahmadian N, Rasta SH, Farhoudi M, Karimi P, Sadigh-Eteghad S (2017) Transcranial low-level laser therapy improves brain mitochondrial function and cognitive impairment in D-galactose–induced aging mice. Neurobiol Aging 58:140–150. https://doi.org/10.1016/j.neurobiolaging.2017.06.025

Salehpour F, Farajdokht F, Erfani M, Sadigh-Eteghad S, Shotorbani SS, Hamblin MR, Karimi P, Rasta SH, Mahmoudi J (2018a) Transcranial near-infrared photobiomodulation attenuates memory impairment and hippocampal oxidative stress in sleepdeprived mice. Brain Res 1682:36–43. https://doi.org/10.1016/j.brainres.2017.12.040

Salehpour F, Farajdokht F, Mahmoudi J, Erfani M, Farhoudi M, Karimi P, Rasta SH, Sadigh-Eteghad S, Hamblin MR, Gjedde A (2019) Photobiomodulation and coenzyme Q_{10} treatments attenuate cognitive impairment associated with model of transient global brain ischemia in artificially aged mice. Front Cell Neurosci 13:74. https://doi.org/10.3389/fncel.2019.00074

Salehpour F, Mahmoudi J, Kamari F, Sadigh-Eteghad S, Rasta SH, Hamblin MR (2018b) Brain photobiomodulation therapy: a narrative review. Mol Neurobiol 55:6601–6636. https://doi.org/10.1007/s12035-017-0852-4

Shirokova N, Niggli E (2013) Cardiac phenotype of Duchenne muscular dystrophy: Insights from cellular studies. J Mol Cell Cardiol 58:217–224. https://doi.org/10.1016/j.yjmcc.2012.12.009

Silva AAO, Leal-Junior EC, D'Avila KAL, Serra AJ, Albertini R, Franca CM, Nishida JA, Carvalho PTC (2015) Pre-exercise low-level laser therapy improves performance and levels of oxidative stress markers in mdx mice subjected to muscle fatigue by high-intensity exercise. Lasers Med Sci 30:1719–1727. https://doi.org/10.1007/s10103-015-1777-7

Silva HNM, Covatti C, Rocha GL, Mizobuti DS, Mâncio RD, Hermes TA, Kido LA, Cagnon VHA, Pereira ECL, Minatel E (2021) Oxidative stress, inflammation, and activators of mitochondrial biogenesis: tempol targets in the diaphragm muscle of exercise trained-mdx mice. Front Physiol 12:649793. https://doi.org/10.3389/fphys.2021.649793

Spencer MJ, Croall DE, Tidball JG (1995) Calpains are activated in necrotic fibers from mdx dystrophic mice. J Biol Chem 270:10909–10914. https://doi.org/10.1074/jbc.270.18.10909

Sundaram JS, Rao VM, Meena AK, Anandaraj MP (2006) Altered expression, intracellular distribution and activity of lymphocyte calpain II in Duchenne muscular dystrophy. Clin Chim Acta 373:82–87. https://doi.org/10.1016/j.cca.2006.05.004

Tanihata J, Nagata T, Ito N, Saito T, Nakamura A, Minamisawa S, Aoki Y, Ruegg UT, Takeda S (2018) Truncated dystrophin ameliorates the dystrophic phenotype of mdx mice by reducing sarcolipin-mediated SERCA inhibition. Biochem Biophys Res Commun 505:51–59. https://doi.org/10.1016/j.bbrc.2018.09.039

Tupling AR (2009) The decay phase of Ca2+ transients in skeletal muscle: regulation and physiology. Appl Physiol Nutr Metab 34:373–376. https://doi.org/10.1139/H09-033

Tupling AR, Bombardier E, Gupta SC, Hussain D, Vigna C, Bloemberg D, Quadrilatero J, Trivieri MG, Babu GJ, Backx PH, Periasamy M, MacLennan DH, Gramolini AO (2011) Enhanced Ca2 þ transport and muscle relaxation in skeletal muscle from sarcolipinnull mice. Am J Physiol Cell Physiol 301:C841–C849. https://doi.org/10.1152/ajpcell.00409.2010

Valduga AH, Mizobuti DS, Moraes FSR, Mâncio RD, Moraes LHR, Hermes TA, Macedo AB, Minatel E (2023) Protection of dystrophic muscle cells using idebenone correlates with the interplay between calcium, oxidative stress and inflammation. Int J Exp Pathol 104:4–12. https://doi.org/10.1111/iep.12463

Vangheluwe P, Schuermans M, Zádor E, Waelkens E, Raeymaekers L, Wuytack F (2005) Sarcolipin and phospholamban mRNA and protein expression in cardiac and skeletal muscle of different species. Biochem J 389:151–159. https://doi.org/10.1042/BJ20050068

Voit A, Patel V, Pachon R, Shah V, Bakhutma M, Kohlbrenner E, McArdle JJ, Dell'Italia LJ, Mendekk JR, Xie L, Hajjar RJ, Duan D, Fraidenraich D, Babu GJ (2017) Reducing sarcolipin expression mitigates Duchenne muscular dystrophy and associated cardiomyopathy in mice. Nat Commun 8:1068. https://doi.org/10.1038/s41467-017-01146-7

Wu KD, Lytton J (1993) Molecular cloning and quantification of sarcoplasmic reticulum $Ca(2^+)$-ATPase isoforms in rat muscles. Am J Physiol Cell Physiol 264:C333–C341. https://doi.org/10.1152/ajpcell.1993.264.2.C333